

## Synchronized Chaos and Spatiotemporal Chaos in Arrays of Coupled Lasers

Herbert G. Winful and Lutfur Rahman

*Department of Electrical Engineering and Computer Science, University of Michigan, Ann Arbor, Michigan 48109*

(Received 25 June 1990)

A subset of lasers in an array of coupled lasers can produce identical, synchronized, chaotic signals. Beyond a critical coupling strength, synchronization fails, and spatiotemporal chaos results. The transition to spatiotemporal chaos is signaled by spatial symmetry breaking. Quantitative measures of the transition from synchronized chaos are provided by Lyapunov exponents, sub-Lyapunov exponents, and the mutual information content.

PACS numbers: 42.50.Tj, 05.45.+b

In this paper we consider the spontaneous emergence of synchronized chaotic signals in a spatially distributed nonlinear system. The model system described here is a semiconductor laser array which serves as a paradigm for the spatiotemporal behavior of coupled nonlinear oscillators. We find that there is a range of coupling strength for which synchronized chaos exists. Outside that range, synchronization breaks down and the system enters a regime of spatiotemporal chaos or turbulence. The loss of synchronization is accompanied by spatial symmetry breaking. We show that the mutual information between two elements of the array is a useful measure of the transition from synchronized chaos to spatiotemporal chaos.

The notion of synchronized chaos may sound, at first, like an oxymoron. Chaotic motion, with its inherent unpredictability and the exponential divergence of nearby trajectories, would seem to preclude the practical realization of identical, synchronized, chaotic signals. In a recent paper, however, Pecora and Carroll have shown that certain subsystems of nonlinear, chaotic systems can be made to synchronize by linking them with common signals.<sup>1</sup> The synchronization results from the influence of a driving (or master) system on a response (or slave) system while the driving system remains unperturbed. The systems considered in Ref. 1 were low-dimensional dynamical systems such as the Lorenz and Rössler equations where spatial effects are irrelevant. On the other hand, some of the most interesting phenomena, such as pattern formation and turbulence, that occur in extended systems involve both the temporal and spatial degrees of freedom. While it is true that a complete description of such phenomena would involve continuous-time, continuous-space models (i.e., partial differential equations), it is remarkable that simple discrete-space models such as cellular automata and lattice dynamical systems exhibit the complicated patterns and spatiotemporal chaos expected of "real" systems.<sup>2</sup> An equally amazing discovery is that some partial differential equation models for spatiotemporal complexity are strictly equivalent to a set of coupled ordinary differential equations corresponding to a finite but high-dimensional system.<sup>3</sup> It is clear that the study of real spatially extended systems that are

accurately described by a finite set of coupled ordinary differential equations will provide insight into the nature of spatiotemporal chaos. This is the motivation for the present work.

Our model system is an array of waveguide lasers coupled by means of their overlapping evanescent fields. In the absence of coupling, each laser operates in a single longitudinal and transverse mode, assumed to be the same for all the lasers. The electric field of the guided mode in the  $j$ th laser is taken as  $E_j(t)e^{-i\omega_0 t}$ , where the complex amplitude  $E_j(t)$  varies slowly compared to the optical frequency  $\omega_0$ . Assuming nearest-neighbor coupling, the evolution of the mode amplitude ( $E_j$ ) and the population ( $N_j$ ) in the  $j$ th laser is described by the equations<sup>4,5</sup>

$$\frac{dE_j}{dt} = \frac{1}{2} \left[ G(N_j) - \frac{1}{\tau_p} \right] (1 - i\alpha) E_j + iK(E_{j+1} + E_{j-1}), \quad (1)$$

$$\frac{dN_j}{dt} = P - \frac{N_j}{\tau_s} - G(N_j)|E_j|^2, \quad (2)$$

where  $G$  is the gain,  $\tau_p$  ( $\sim 1$  ps) is the photon lifetime,  $\tau_s$  ( $\sim 2$  ns) is the lifetime of the active population,  $P$  is the pump rate, and  $K$  is the coupling strength between adjacent lasers. The parameter  $\alpha$  is known as the linewidth enhancement factor in semiconductor lasers and is a measure of the carrier-density-dependent refractive index. For operation not too far from the lasing threshold of the uncoupled lasers, the gain may be expressed as  $G(N_j) = G(N_{th}) + g(N_j - N_{th})$ , where  $N_{th}$  is the carrier density at threshold,  $G(N_{th}) = 1/\tau_p$ , and  $g = \partial G/\partial N$  is the differential gain. It should be noted that if the population  $N_j$  is adiabatically eliminated, Eq. (1) represents a set of coupled van der Pol oscillators and is also identical to the discrete Ginzburg-Landau equation which has been used often as a model for spatiotemporal complexity.<sup>6</sup>

It is convenient to transform Eqs. (1) and (2) into dimensionless form for the normalized magnitude ( $X_j$ ) and phase ( $\phi_j$ ) of the electric field, and the normalized excess carrier density  $Z_j$  in the  $j$ th laser. These equa-

tions are<sup>5</sup>

$$\dot{X}_j = Z_j X_j - \eta [X_{j+1} \sin(\phi_j - \phi_{j+1}) - X_{j-1} \sin(\phi_{j-1} - \phi_j)], \quad (3)$$

$$\dot{\phi}_j = \alpha Z_j - \eta [(X_{j+1}/X_j) \cos(\phi_j - \phi_{j+1}) + (X_{j-1}/X_j) \cos(\phi_{j-1} - \phi_j)], \quad (4)$$

$$T \dot{Z}_j = p - Z_j - (1 + 2Z_j) X_j^2, \quad j = 1, 2, \dots, N, \quad (5)$$

with  $X_0 = X_{N+1} = 0$ . Here the overdots signify derivatives with respect to a reduced time  $t/\tau_p$  and we define the following variables and parameters:

$$X_j = (\frac{1}{2} g \tau_c)^{1/2} |E_j|, \quad Z_j = \frac{1}{2} g N_{th} \tau_p (N_j/N_{th} - 1),$$

$$p = \frac{1}{2} g N_{th} \tau_p (P/P_{th} - 1), \quad \eta = K \tau_p, \quad T = \tau_c/\tau_p.$$

Equations (3)-(5) represent an oscillator assembly which in the absence of coupling ( $\eta = 0$ ) would evolve toward a steady state with  $Z_j = 0$ ,  $X_j = \sqrt{p}$ , and arbitrary phases  $\phi_j$ . For nonzero coupling, the array of lasers can organize itself into a macroscopically coherent structure with well-defined phase relationships between the oscillators.

The self-organizing principle underlying the collective behavior of coupled oscillators is that of synchronization or mutual entrainment.<sup>6</sup> For the laser array in this discussion, there are two levels of synchronization involved. The first represents a quiescent state in which the amplitudes  $X_j$  and carrier densities  $Z_j$  are constant in time while the phases  $\phi_j$  evolve linearly in time at the same rate (possibly zero) for all the lasers. For weakly coupled lasers ( $\eta \leq 10^{-5}$ ), the stable phase-locked or quiescent state is one in which the amplitude distribution across the array is nearly uniform. If this were not the case, local regions of high field would result (through the  $\alpha$  parameter) in detunings between the lasers thereby destabilizing phase locking. This uniform phase-locked state, however, is not always stable. Above a critical coupling strength the quiescent state loses stability

through a supercritical Hopf bifurcation.<sup>5</sup> Physically, the delayed response of the carriers leads to phase lags between the oscillators and destroys phase locking. The dynamical variables—amplitudes, phases, and carrier densities—all pulsate in time. The pulsations that occur in different elements of the array may be in time step with each other, and this represents the second level of synchronization.

To elucidate the notion of synchronized chaos, consider the case of three identical coupled lasers. The presence of a spatial grid imposes a spatial symmetry and makes it possible to determine *a priori* which elements in the array are likely to synchronize. In the stable phase-locked state, symmetry dictates that  $X_1 = X_3$ . For this particular case, stable quiescent states exist for  $\eta < 10^{-4.43}$ . As  $\eta$  is increased beyond this value, the branch of phase-locked solutions loses stability in favor of a self-pulsing solution. The spatial symmetry, however, is maintained in the sense that the pulsations in  $X_1$  and  $X_3$  are synchronous. As  $\eta$  is increased further, a sequence of period-doubling bifurcations occurs at  $\eta = 10^{-3.578}, 10^{-3.541}, 10^{-3.534}$ , etc. Throughout this bifurcation sequence, lasers 1 and 3 remain synchronized with each other, i.e.,  $X_1 = X_3, \phi_1 = \phi_3, Z_1 = Z_3$ .

For  $\eta = 10^{-3.5}$ , the temporal evolution of the output of each laser in the array is chaotic. The computed Lyapunov spectrum is  $(+6.1, 0, 0, -2.1, -2.3, -2.4, -3.8, -4.0, -13.0) \times 10^{-4}$ . These Lyapunov exponents are the eigenvalues of the Jacobian of the evolution equations averaged along an orbit of the system and hence provide a measure of the average exponential divergence of nearby orbits. The presence of a positive Lyapunov exponent confirms that the evolution is indeed chaotic. It is remarkable, however, that the temporal evolution of the output intensities in lasers 1 and 3 are identical, as shown in Fig. 1(a). This is the regime of synchronized chaos as can be seen [Fig. 1(b)] in the projection of the flow onto the  $X_1$ - $X_3$  plane. In the  $X_1$ - $X_2$  plane, it is clear that the motion is along a strange at-

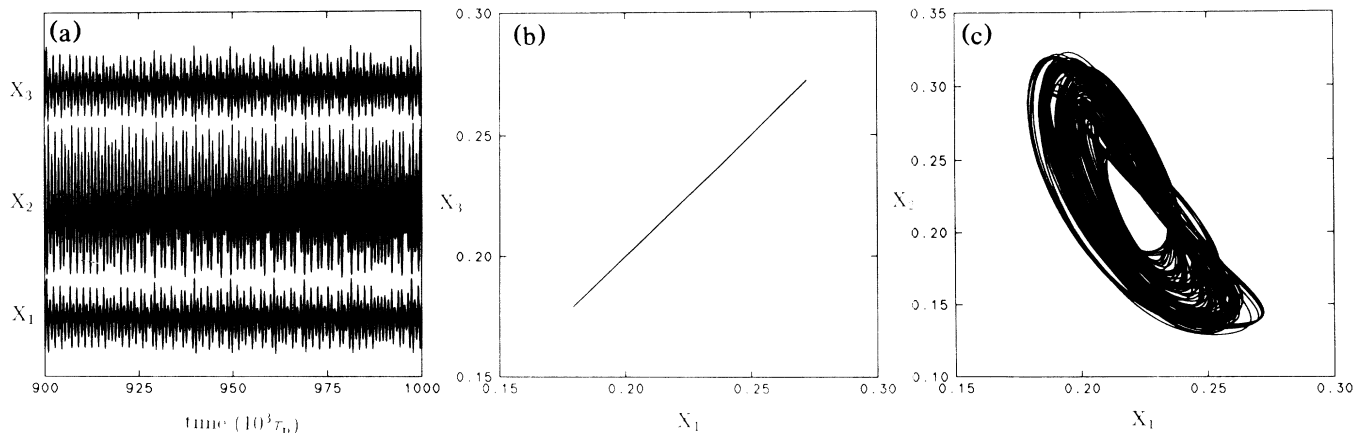


FIG. 1. Synchronized chaos for  $\eta = 10^{-3.5}$ . (a) Time series for the amplitudes  $X_1, X_2$ , and  $X_3$ ; (b) projection of the flow onto the  $X_1$ - $X_3$  plane; (c) projection onto the  $X_1$ - $X_2$  plane. Parameter values are  $p = 0.05$ ,  $T = 2 \times 10^3$ , and  $\alpha = 5$ .

tractor [Fig. 1(c)]. The regime of synchronized chaos thus corresponds to spatial order and temporal chaos.

Pecora and Carroll<sup>1</sup> have introduced the notion of sub-Lyapunov exponents to quantify the ability of chaotic subsystems to synchronize. If the sub-Lyapunov exponents are all negative, the subsystems will synchronize. We apply this concept to the mutual entrainment of lasers 1 and 3 and find that the sub-Lyapunov exponents associated with the subspace  $(X_1, \phi_1, Z_1)$  are  $(-2.1, -2.3, -2.5) \times 10^{-4}$  in the region of synchronized chaos.

The presence of spatial symmetry does not guarantee synchronization of chaotic orbits. When the coupling strength  $\eta$  is increased to  $10^{-30}$ , synchronization breaks down. Figure 2(a) now shows the evolution of  $X_1$ ,  $X_2$ , and  $X_3$  as a function of time. There is now no apparent relationship between  $X_1$  and  $X_3$ . The spatial order has been lost. This spatial symmetry breaking is also evident in Fig. 2(b) where we show the projection of the flow onto the  $X_1$ - $X_3$  plane. The attractor here is a complicated tangle. Figure 2(c), the projection in the  $X_1$ - $X_2$  plane, shows that its structure is much more complex than in the case of synchronized chaos. This is the regime of spatiotemporal chaos. The Lyapunov spectrum associated with this evolution is  $(+30.9, +12.8, +0.4, 0, -0.8, -3.4, -5.7, -17.2, -33.6) \times 10^{-4}$ . The system is now hyperchaotic, with more than one positive Lyapunov exponent. The associated sub-Lyapunov exponents are  $(+7.3, -2.0, -11.5) \times 10^{-4}$ . Since these sub-Lyapunov exponents are not all negative, synchronization cannot occur for this chosen value of coupling.

Intuition suggests that the chaos seen in Fig. 2 is higher dimensional than that of Fig. 1. To quantify this intuition we calculate the Lyapunov dimension associated with the attractors shown. The Lyapunov dimension is a measure of the number of phase-space variables needed to accurately capture the dynamics. It is defined as<sup>7</sup>

$$D_L = j + (\lambda_1 + \lambda_2 + \dots + \lambda_j) / |\lambda_{j+1}|,$$

where the  $\lambda_i$  are arranged such that  $\lambda_1 \geq \lambda_2 \geq \lambda_3$ , etc., and  $j$  is the largest integer such that  $\lambda_1 + \lambda_2 + \dots + \lambda_j \geq 0$ . In the region of synchronized chaos the Lyapunov dimension is  $D_L = 5.7$  which suggests that the evolution of the system occurs in a space of dimension no greater than 6. The dynamics of the three-laser system is then identical to that of two lasers with asymmetrical coupling. In the regime of spatiotemporal chaos ( $\eta > 10^{-30}$ ) the Lyapunov dimension  $D_L$  is 8.5. This implies that the system explores essentially the entire nine-dimensional phase space available to it.

The transition from synchronized chaos to spatiotemporal chaos can be further characterized by means of the mutual information  $M_{xy}$  which measures the general dependence of two variables  $x$  and  $y$ . The mutual information is defined in terms of Shannon entropy in the following manner.<sup>8</sup> Consider a dynamical variable  $x(t)$  that depends continuously on time  $t$ . One starts by dividing the possible range of  $x$  into  $N$  boxes of size  $\epsilon$ . The state  $x$  is measured at intervals of time  $t$ . Let  $P(x_i)$  be the probability that  $x$  lies in the  $i$ th box. Then the entropy of  $x$  is defined as

$$H_x = - \sum_{i=1}^N P(x_i) \log_2 P(x_i).$$

A similar quantity exists for dynamical variable  $y$ . The amount of information (in bits) about  $x$  contained in  $y$ , or vice versa, is given by the mutual information

$$M_{xy} = H_x + H_y - H_{xy},$$

where  $H_{xy}$  is the joint entropy defined in terms of the joint probability  $P(x_i, y_j)$  of  $x$  lying in the  $i$ th box and  $y$  lying the  $j$ th box:

$$H_{xy} = - \sum_{i,j=1}^N P(x_i, y_j) \log_2 P(x_i, y_j).$$

Mutual information has the convenient property that it vanishes if  $x$  and  $y$  are independent and is large if the two variables are correlated.

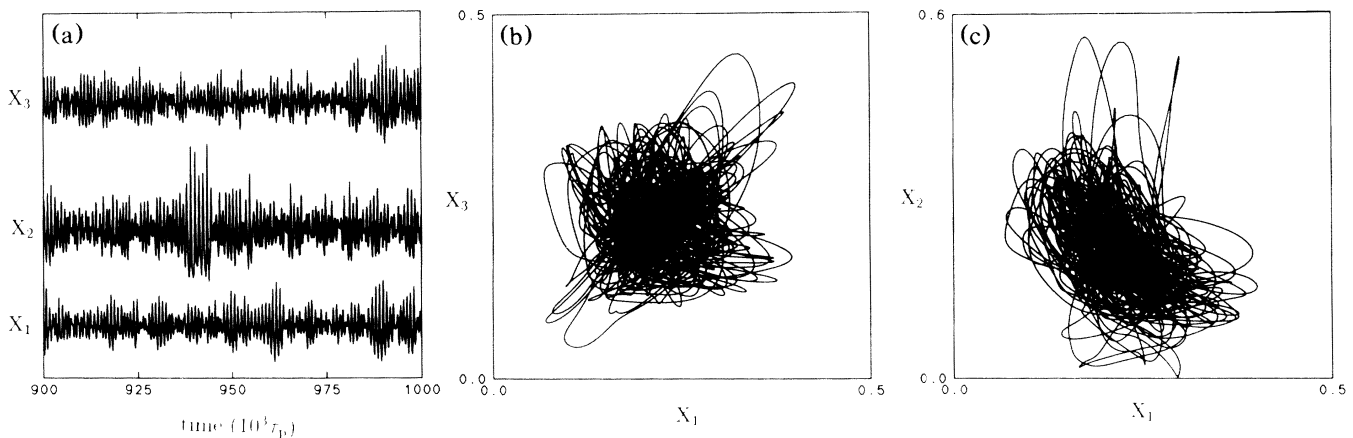


FIG. 2. Spatiotemporal chaos for  $\eta = 10^{-30}$ . (a) Time series for the amplitudes  $X_1$ ,  $X_2$ , and  $X_3$ ; (b) projection of the flow onto the  $X_1$ - $X_3$  plane; (c) projection onto the  $X_1$ - $X_2$  plane. Except for  $\eta$ , the parameter values are the same as in Fig. 1.

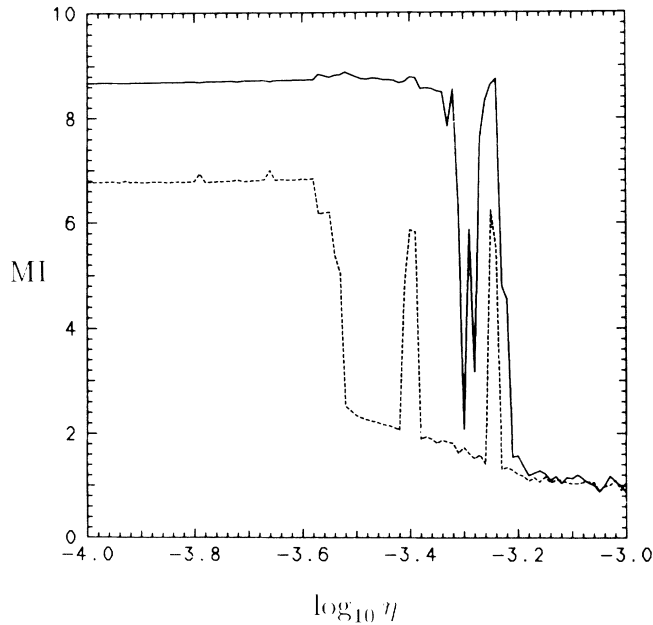


FIG. 3. Mutual information vs coupling strength. Solid curve:  $M_{13}$  (mutual information of lasers 1 and 3). Dashed curve:  $M_{12}$  (mutual information of lasers 1 and 2).

Figure 3 shows  $M_{13}$  (mutual information between elements 1 and 3) and  $M_{12}$  (mutual information between elements 1 and 2) plotted as a function of  $\eta$ . For  $\eta < 10^{-3.6}$  both  $M_{13}$  and  $M_{12}$  are high, indicating the strong correlation that exists among all three oscillators just beyond the first Hopf bifurcation. The sharp drop in  $M_{12}$  that occurs in the vicinity of  $\log_{10}\eta \cong -3.6$  signifies the period-doubling bifurcations to chaos. There is a region between  $\log_{10}\eta \cong -3.6$  and  $-3.3$  where  $M_{12}$  is low but  $M_{13}$  remains high. This is the region of synchronized chaos where the system is temporally chaotic but maintains a high degree of spatial order. The peaks in  $M_{12}$  in the vicinity of  $\log_{10}\eta \cong -3.40$  and  $-3.24$  identify periodic windows within the chaotic region. Finally, beyond  $\log_{10}\eta \cong -3.15$  both  $M_{13}$  and  $M_{12}$  are low. In this region, the system is disordered in both space and time. Mutual information thus provides a measure of the qualitative changes in the spatiotemporal dynamics as a control parameter of the system is varied.

The phenomena discussed here are quite robust. Synchronized chaos persists even when the coupled lasers are

not quite identical. It occurs over a wide range of initial conditions and has also been seen in larger oscillator assemblies. However, the computation of Lyapunov exponents and dimensions for the larger arrays is extremely time consuming and will be reported elsewhere.

In conclusion, we have demonstrated that synchronized chaotic time series can be generated spontaneously in a spatially distributed system. The synchronization is mutual in the sense that the subsystems affect each other and one cannot identify a master or slave component. Synchronization is possible only within a range of coupling strengths. When synchronization breaks down we observe spatiotemporal chaos. These results may have relevance in other areas of science where coupled nonlinear oscillators are used to model self-organization and spatiotemporal complexity.

The authors acknowledge illuminating discussions with Chris Langton of Los Alamos National Laboratory and Al Hero of the University of Michigan. This research is partially supported by the National Science Foundation through a Presidential Young Investigator Award (H.G.W.) and through Grant No. ECS-8906214. Additional support it provided by the ARO under the URI program.

<sup>1</sup>L. M. Pecora and T. L. Carroll, Phys. Rev. Lett. **64**, 821 (1990).

<sup>2</sup>J. P. Crutchfield and K. Kaneko, in *New Directions in Chaos*, edited by Hao Bai-Lin (World Scientific, Singapore, 1987).

<sup>3</sup>J. M. Hyman and B. Nicolaenko, Physica (Amsterdam) **18D**, 113 (1986).

<sup>4</sup>S. S. Wang and H. G. Winful, Appl. Phys. Lett. **52**, 1774 (1988).

<sup>5</sup>H. G. Winful and S. S. Wang, Appl. Phys. Lett. **53**, 1894 (1988).

<sup>6</sup>K. Kuramoto, *Chemical Oscillations, Waves, and Turbulence* (Springer-Verlag, New York, 1984).

<sup>7</sup>J. Kaplan and J. Yorke, in *Functional Differential Equations and Approximation of Fixed Points*, edited by H. O. Peitgen and H. O. Walther (Springer-Verlag, Heidelberg, 1979).

<sup>8</sup>A. M. Fraser and H. L. Swinney, Phys. Rev. A **33**, 1134 (1986).